Available online at **www.joac.info**

ISSN: 2278-1862

Journal of Applicable Chemistry

2020, 9 (3): 404-420

(International Peer Reviewed Journal)

Electrochemical Study on the Affectivity of Omeprazole Drug as an Inhibitor for Corrosion of High Carbon Steel in 1M HCl

A. S. Fouda[1]*, S. M. Rashwan[2], H. Ibrahim[2] and R.M. Ahmed[1]

1. Chemistry Department, Faculty of Science, Mansoura University, Mansoura-35516, **EGYPT**
2. Department of Chemistry, Faculty of Science, Suez Canal University, **EGYPT**

Email:asfouda@hotmail.com

Accepted on 8th May, 2020

ABSTRACT

A pharmaceutically active compound of Omeprazole (OME) is a proton pump inhibitor drug that protect stomach acid discharge. OME was investigated as organic corrosion inhibitor for high carbon steel (HCS) in 1 M HCl utilizing electrochemical impedance spectroscopy (EIS), potentiodynamic polarization (PP), electrochemical frequency modulation (EFM) and mass loss methods. The impact of EIS displayed the increase in the polarization resistance (R_P) and the decline in the double layer capacitance (C_{dl}). Polarization data demonstrated that, this OME goes about as mixed-type inhibitor. Inhibition efficiency was dependent on doses of OME and temperature. The adsorption of this extract on the outside of HCS from the damaging corrosive medium has been found to obey Langmuir adsorption isotherm. The thermodynamic parameters of HCS consumption in 1M HCl were computed and discussed. The AFM examination of the HCS surface indicated that the concentrate avoided consumption by adsorption on its surfaces and reduced the roughness. FTIR results showed that the inhibition mechanism was by adsorption process, through the functional groups present in the drug component. Results obtained indicate the potential utilization of this drug as corrosion inhibitor for HCS in acidic media.

Graphical Abstract

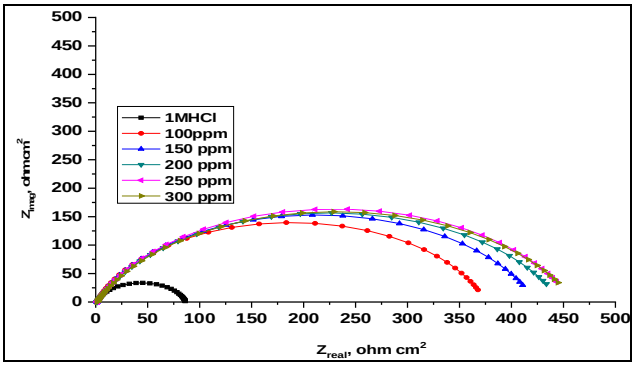

Nyquist plots without and with altered OME concentrations for HCS dissolution in corrosive solution

Keywords: Acidic inhibition, High Carbon steel (HCS), Omeprazole (OME), EFM, EIS.

INTRODUCTION

Omeprazole [1] was purchased from medicine shop as a trade name Omeprazole. It can be taken by mouth as capsules, tablets as oral liquid suspension or by injection into a vein. [2, 3] OME works on gastric parietal cells to irreversibly protect (H+/K+)-ATPase functions and suppresses the creation of gastric acid [4]. It works by lowering the quantity of acid your stomach kinds [5]. OME can be utilized in the treatment of gastroesophageal reflux disease (GERD) [6, 7] .OME may also be utilized in amalgamation with antibiotics to flimsiness ulcers produced by Helicobacter pylori [8, 9] OME be appropriate to a class of drugs recognized as proton pump protector (PPIs) [10]. Corrosion is a huge procedure assuming a significant role in economic and man-factory, particularly for metals. The utilization of inhibitors is one of the most genuine techniques for hindrance against corrosion in acidic media [11]. Most organic protection acting by adsorption on the metal surface most notable on corrosive medium is organic composite containing nitrogen , sulfur, and oxygen molecules. Among them organic inhibitors are many advantages such as high hindrance productivity [12-15]. Organic heterocyclic composite has been utilized for the corrosion restraint of iron [16-19], copper [20], aluminum [21-23], and different metals [24, 25] in various corrosive media. Although many of these composites have high restraint efficiencies, several have undesirable reactions, even in very small concentrations, due to their toxicity to humans, deleterious environmental effects, and high cost [26]. Most of the pharmaceutical active substances are far more expensive, miscibility high in water, safe utilize, big molecular size than the organic inhibitors currently implemented. Therefore, our study was focused on the usage of expired drugs (OME) or unused drugs because of patient's non-compliance that contain in their composition active substances with inhibitory properties. The use of unused drugs can solve two problems: limitation of the environmental pollution with pharmaceutically active compounds and reduction of the disposal costs of expired drugs.

MATERIALS AND METHODS

Composition of HSC samples: Carbon steel is an alloy consisting of iron and carbon. Numerous other elements are acceptable in carbon steel, with small maximum percentages. The HCS sample conformation in weight % is: 0.55%-0.95% C, with 0.30%-0.90% Mg. It is very strong and holds shape memory well, making it ideal for springs and wire [27].

Materials and Solutions: HCS alloy specimens were utilized. The aggressive medium used is HCl 37%. Solutions of 1.0 M HCl had prepared by dilution with distilled water. The OME stock solution 10^3 ppm was used to prepare (100, 150, 200, 250 and 300 ppm). The structure of OME is shown in (Figure 1).

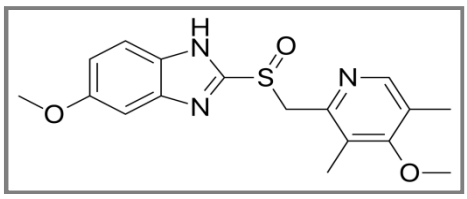

Figure 1. The structure of OME (6-Methoxy-2-(4-methoxy-3, 5-dimethyl-pyridin-2-yl-methanesulfinyl)-1H-benzoimidazole)

Mass loss (ML) method: The coins with size (2 × 2 × 0.2 cm) x2 were dipped in 100 mL of 1M HCl and existences of the various contents of OME are set in water thermostat. After 3 h the samples were removed, rinsed, dried, and weighed again. The % IE and the θ were founded from Eq. (1) [27],

$$IE\% = \theta \times 100 = \left[1 - \frac{W}{W^{\circ}}\right] \times 100 \qquad \ldots(1)$$

Where, W^{o} and W are the values of the average weight loss without and with addition of the inhibitor respectively.

Potentiodynamic polarization (PP) method: All electrochemical experiments were performed at 25°C using three-electrode cell setup consists of (SCE) a saturated calomel electrode utilizes as electrode reference, (Pt) platinum wire utilize as an electrode counter and HCS as (WE) working electrode. The WE were prepared as follows at first one side of HCS sheet (10 ml x 10 ml x 20 ml) has fused to a copper wire for electrical connection [28]. Subsequently, the copper wire that attached to HCS sheet was inserted into a glass tube and then fixed by epoxy resin to make the size of HCS visible to the test solutions is 1 cm^2. The potential range was (-1.1 to – 0 V vs. SCE) at OCP with a scan rate 1 mVs^{-1}. The (i_{corr}) was used for calculation of (IE %) and (θ) as in balance 2:

$$IE\ \% = \Theta \times 100 = \left[1 - \frac{i_{corr(inh)}}{\mathrm{i}corr_{(free)}}\right] \times 100 \qquad \ldots(2)$$

Where, $i_{corr(free)}$ and $i_{corr(inh)}$ are the corrosion current in the lack and attendance of OME, correspondingly .

Electrochemical impedance spectroscopy (EIS) method: This technique was done by AC signs of 5 mV peak to peak amplitude and at frequency range of 10^7 Hz to 0.1 Hz. The (% IE) and θ were founded from eq. (3):

$$IE\% = \Theta \times 100 = \left[1 - \left(\frac{R^{\circ}_{ct}}{R_{ct}}\right)\right] \times 100 \qquad \ldots(3)$$

Where, R^{o}_{ct} and R_{ct} are the charge transfer resistance without and with OME, individually.

Electrochemical frequency modulation (EFM) method: This technique used two frequencies of range 2 and 5 Hz depended on three conditions. The (i_{corr}), (β_c and β_a) and (CF-2, CF-3) (Causality factors) were measure by the greater two peaks [29]. The electrode potential could stabilize 30 min before starting the measurements. All the experiments were conducted at 25°C .

All electrochemical tests were achieving utilizing Gamry Instrument (PCI4/750) Potentiostat/ Galvanostat/ZRA. This contains a Gamry framework system constructed on the ESA 400. Gamry uses contain DC105 software for PP, EIS 300 software for EIS, and EFM 140 software for EFM measurements via computer for collecting data. E_{chem} Analyst 6.03 software was utilized for plotting, graphing, and fitting data.

Surface examinations: HCS Coins utilized for surface analysis were dipped in 1.0 M HCl in the nonexistence and existence of 300ppm of OME solutions for 24 h. After the immersion time, the coins had removed then splashed with bidistilled water many times to remove any residue and dried. The investigation was done utilizing scanning electron microscope (JOEL 840, Japan) (SEM), atomic force microscope (AFM). FTIR analyses had tested for HCS surface before and after immersion 3h in 300 ppm of OME and then compared to the spectra of OME. FTIR is utilized to investigate the film designed on the surface of HCS by Thermo Fisher Nicolet IS10, USA in the spectral range of 400-4000 cm^{-1}.

RESULTS AND DISCUSSION

Mass loss (ML) method: The reduction in mass of HCS alloy can be studied in occurrence of OME at 30°C. Figure 2 shows that OME decreases the mass reduction and therefore corrosion rate. The (%IE) and then θ, of the OME for the HCS were founded by eq. (1). The values of %IE are given in (Tables 1, 2). From these tables, it is illustrious that the IE% improve steadily with improving the dose of omeprazole and lower with temperature rising from 30-50°C.

The noted protection activity of the OME could ascribed to the adsorption of OME molecule on HCS surface. The coated layer of the adsorbed atoms must have isolated the metal surface of the HCS

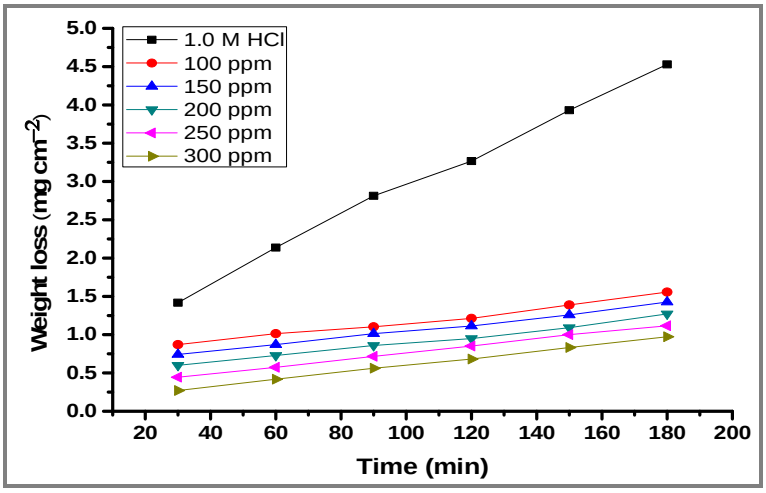

Figure 2. Time-ML curve for the corrosion of HCS in 1 M HCl without and using various OME doses at 30°C.

Table 1. The corrosion rate (C.R.) in (mg cm^{-2} min^{-1}) and IE data gotten from ML test without and utilizing various OME doses at 30°C

Conc., ppm	ML, mg cm^{-2}	C.R., mg cm^{-2} min^{-1}	Θ	%IE
1 M HCl	4.729	0.0390	---	---
100	1.296	0.0057	0.803	80.3
150	0.684	0.0042	0.833	83.3
200	0.456	0.0038	0.877	87.7
250	0.336	0.0028	0.896	89.6
300	0.324	0.0027	0.945	94.5

Table 2. Parameters such as %IE, (***θ***) and (C.R.) for HCS alloy dissolution after 120 min without and using various OME doses at 30-50°C

Conc., ppm	Temp., °C	C.R., (mg cm^{-2}min^{-1})	Θ	%IE
	30	0.0057	0.803	80.3
	35	0.0071	0.789	78.9
100	35	0.0079	0.741	74.1
	45	0.0100	0.700	70.0
	50	0.0108	0.633	63.3
	30	0.0042	0.833	83.3
	35	0.0058	0.803	80.3
150	35	0.0077	0.779	77.9
	45	0.0093	0.742	74.2
	50	0.0100	0.660	66.0
	30	0.0038	0.877	87.7
	35	0.0052	0.849	84.9
200	35	0.0061	0.813	81.3
	45	0.0083	0.785	78.5
	50	0.0098	0.709	70.9
	30	0.0028	0.896	89.6
	35	0.0048	0.887	88.7
250	35	0.0056	0.839	83.9
	45	0.0067	0.815	81.5
	50	0.0078	0.740	74.0
	30	0.0027	0.945	94.5
	35	0.0033	0.918	91.8
300	35	0.0039	0.864	86.4
	45	0.0046	0.854	85.4
	50	0.0054	0.792	79.2

from the aggressive medium which limited the dissolution of the latter by blocking of their corrosion sites and hence diminishing the corrosion rate; with raising efficiency as their doses were increased.

Potentiodynamic polarization (PP) method: Tafel curves of HCS electrode in 1 M HCl with and without altered contents of OME can be studied from (Figure 3). From the data of (Table 3) OME has effect on both of cathodic and anodic processes and the IE rises with increasing of the OME content. E_{corr} was a little changed, representative that OME acts as a mixed–kind inhibitor [**31-33**]. i_{corr} reduced through the OME addition to 1M HCl. % IE and (θ) were calculated from eq. (2):

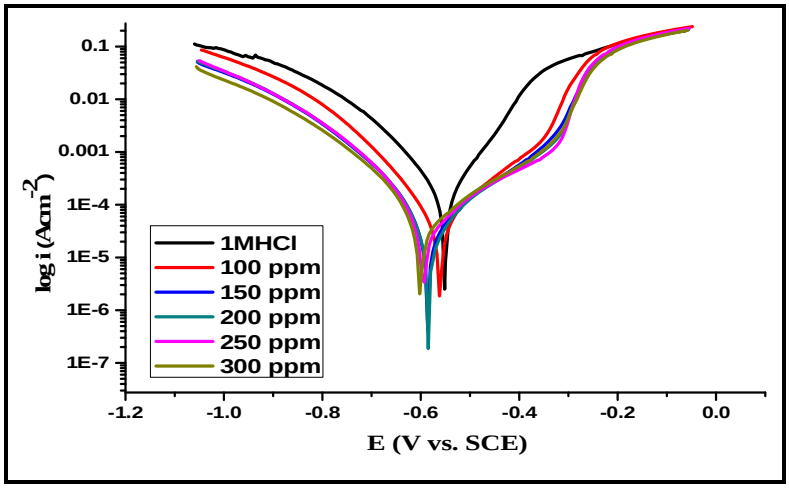

Figure 3. Polarization curves of the HCS dissolution with and without altered doses of OME at 25°C.

Table 3. PP results of HCS dissolution with and without different doses of OME at 25°C

Conc., ppm	i_{corr}, µA cm^{-2}	$-E_{corr}$, mV vs. SCE	β_a, $mVdec^{-1}$	$-\beta_c$, $mVdec^{-1}$	C.R., mm y^{-1}	θ	%IE
1 M HCl	129.0	551	77	86	59.1	--	--
100	23.5	561	60	59	10.7	0.818	81.8
150	21.1	586	80	44	9.6	0.836	83.6
200	19.2	585	90	55	8.7	0.851	85.1
250	16.4	595	92	50	7.5	0.873	87.3
300	11.4	601	53	26	5.1	0.912	91.2

Electrochemical impedance spectroscopy (EIS) method: (Figure 4 and 5) present the Nyquist and Bode plots for HCS dissolution in corrosive solution without and with altered OME doses. The Nyquist diagrams do not display ideal semicircle, this referred to the frequency dispersion [**28-32**] which results from the surface roughness [**33**]. In corrosive solution without and with OME, the diagrams show the same capacitive loop, but its diameter increases with rise OME dose. The impedance spectrum was analyzed by using the simple equivalent circuit model shown in (Figure 6). The circuit has the solution resistance R_s and the double layer capacitance C_{dl} that putted parallel to R_{ct} [**34**]. The double layer capacitances, C_{dl}, for a circuit including a CPE parameter (Y_0 and n) were calculated from the following equation [**35-37**]:

$$C_{dl} = Y_0 (\omega_{max})^{n-1} \quad \ldots(4)$$

$$\Omega_{max} = 2\pi f_{max} \quad \ldots(5)$$

Where, Y_0 = the CPE degree and f_{max} is the frequency at which the imaginary constituent of the EIS is greatest.

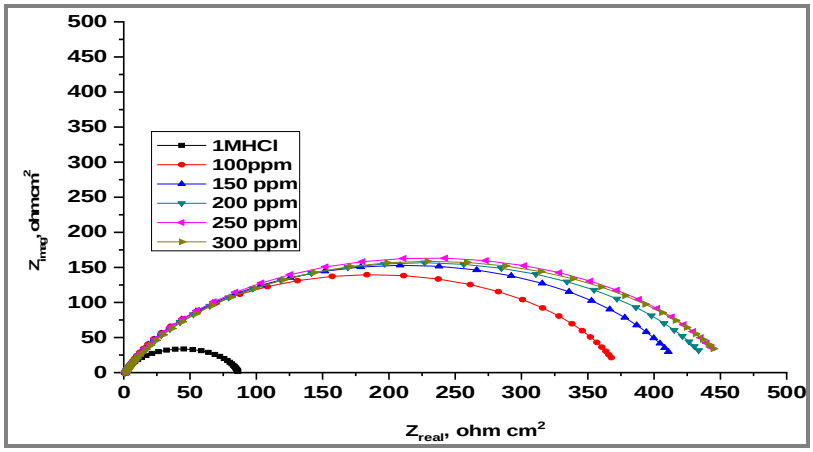

Figure 4. Nyquist plots without and with altered OME concentrations for HCS dissolution in corrosive solution.

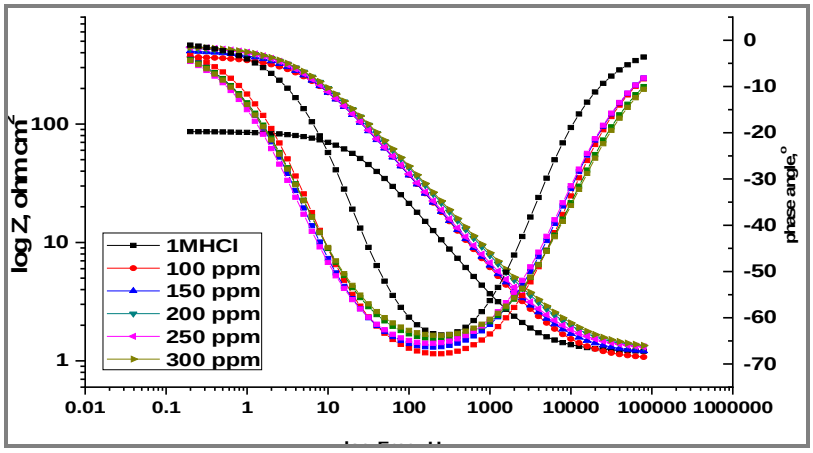

Figure 5. Bode plots recorded for HCS in 1 M HC1 without and with various dose of OME at 25°C.

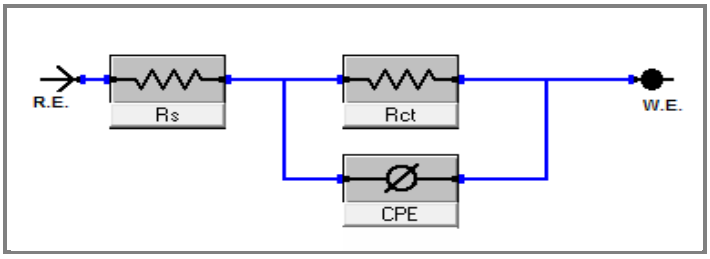

Figure 6. The circuit used in EIS results.

Table 4. EIS results without and with different OME doses for HCS dissolution in corrosive solution

Conc., ppm.	R_{ct}, Ω cm^2	Yo x10^{-6}	C_{dl}, x10^{-6} µF cm^{-2}	θ	% IE
1M HCl	89.5	153	84.1	---	---
100	374.3	136	79.8	0.761	76.1
150	421.9	155	77.9	0.788	78.8
200	446.4	150	73.5	0.799	79.9
250	490.2	155	70.4	0.817	81.7
300	544.7	160	69.9	0.836	83.6

It includes the obtained impedance data (Table 4). As shown, R_{ct} increases, and hence %IE increases, with the increase in OME concentration, while C_{dl} decreases. That is because the adsorption of the OME on the HCS surface, forming a film on it. The inhibition efficiency is calculated from the charge–transfer resistance data as shown in equation 3 [38-41].

Electrochemical frequency modulation (EFM) method: EFM is characterized by speed and greatly accuracy in calculating the current data [42-43]. (Figure 7) indicates the EFM of HCS in 1.00M HCl solution and altered dose of OME. The EFM parameters such as (CF-2 and CF-3), (β_c and β_a) and (i_{corr}) can be measured from the higher current peaks. The CF is closer to the standard data proved the validity of the calculated data [44]. The IE% increase with the raising of OME concentrations and was calculated as follows:

$$IE\ \%_{EFM} = \left(1 - \frac{i_{corr}}{i^{\circ}_{corr}}\right) \times 100 \quad \ldots(5)$$

Where, i^{o}_{corr} and i_{corr} are corrosion current densities in the absence and presence of OME, individually (Table 5).

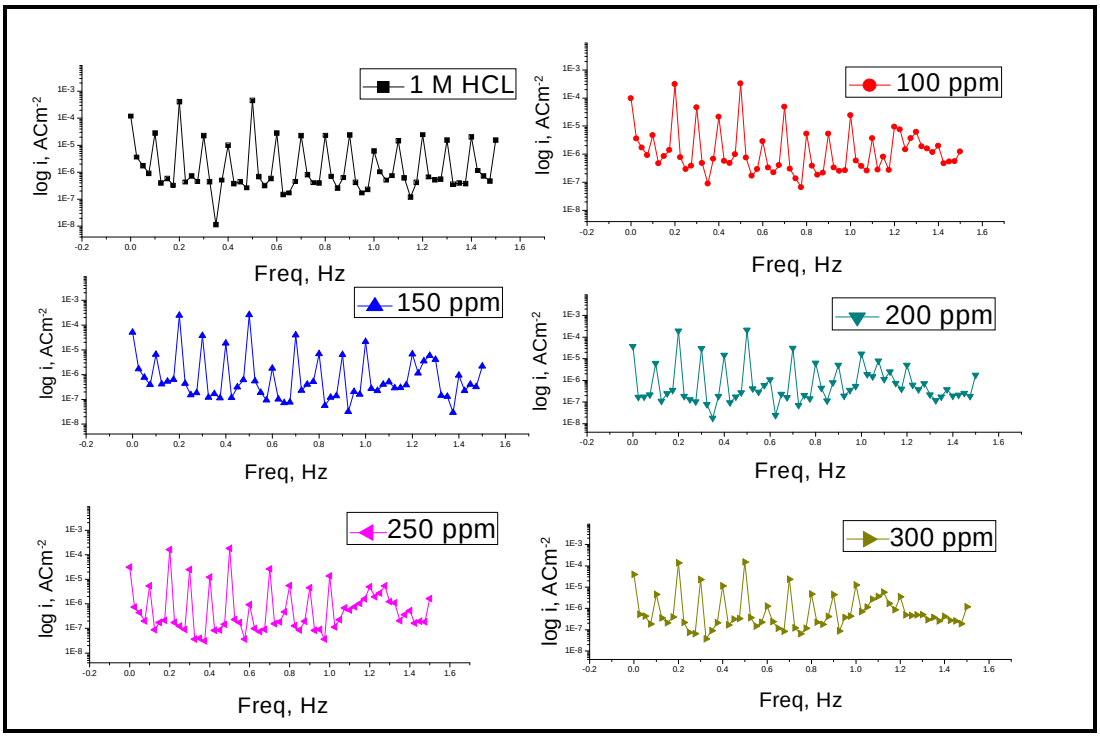

Figure 7 (a-g). EFM spectra for HCS in corrosive solution in without and with altered doses of OME.

Table 5. EFM results without and with different OME doses for HCS dissolution in corrosive solution at 25°C.

Conc, ppm	i_{corr}, µA	Ba mV dec^{-1}	βc mV dec^{-1}	C.R. mpy	CF-2	CF-3	Θ	%IE
1 M HCl	284.7	36	64	130	1.7	2.8	---	---
100	76.7	144	152	35	1.6	2.2	0.731	73.1
150	70.6	147	174	32	2.8	3.7	0.752	75.2
200	61.7	129	144	28	2.6	3.2	0.783	78.3
250	51.5	105	114	23	2.1	3.1	0.819	81.9
300	31.1	87	72	14	2.3	3.1	0.891	89.1

Adsorption Isotherms: Several isotherms had used to fit data [45], but the maximum fit was achieved to follow Langmuir adsorption isotherm which was shown in (Figure 8) for the OME drug. Langmuir measured from the following relation [46]:

$$\frac{C}{\theta} = \frac{1}{K} + C \qquad \ldots(6)$$

Where the concentration of the OME expressed as *C*, the adsorptive equilibrium constant expressed as *K* and can be computed from the intercept of the difference among the *C/ Θ* and C in (Figure 8), the variation between *C/ Θ* and C where *Θ* is the surface coverage, = *IE/100*.
The ΔG°_{ads} and K_{ads} data are in (Table 6) the ΔG^{o}_{ads} founded by**:**

$$\Delta G^{o}_{ads} = - RT \ln (55.5\ K_{ads}) \qquad \ldots(7)$$

The OME adsorption is spontaneous and this is proven by the ΔG°_{ads} negative sign. From the data of ΔG^{o}_{ads} (around to -20 kJ mol^{-1}), proven that the OME adsorption is physisorption. Vant't Hoff equation can be used to measure ΔH°_{ads} [47] expressed by:

$$\text{Ln } K_{ads} = \frac{-\Delta H^{\circ}_{ads}}{RT} + const \qquad \ldots(8)$$

And eq. (9): can be used to calculate ΔS^{o}_{ads}

$$\Delta G^{o}_{ads} = \Delta H^{o}_{ads} - T\ \Delta S^{o}_{ads} \qquad \ldots(9)$$

(Figure 9) shows the relation between Lin K_{ads} and 1000/T. A negative sign of ΔS^{o}_{ads} proved that the disorder of corrosion process is decreases by using OME (Table 6) [48].

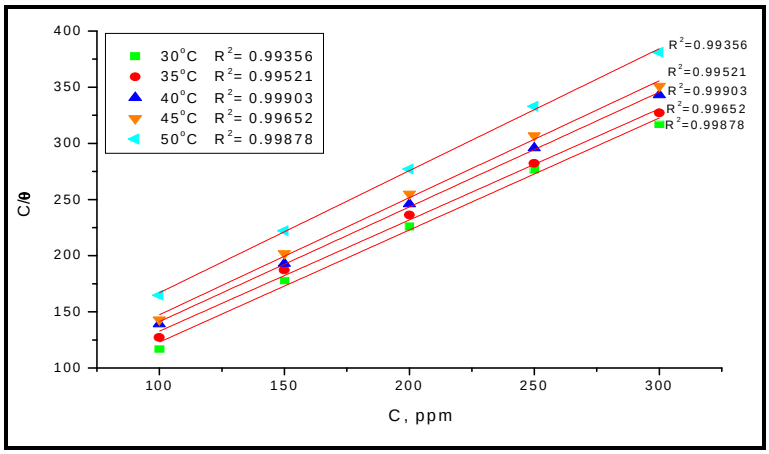

Figure 8. Langmuir adsorption bends for HCS in 1.00 M HCl containing altered dose of OME at 303-318K.

Table 6. Langmuir data for HCS without and using various OME doses at (30°C-50°C)

Temp., K	K_{ads} x10^{-3} M^{-1}	$-\Delta G^{\circ}_{ads}$ kJ mol^{-1}	$-\Delta H^{\circ}_{ads}$ kJ mol^{-1}	$-\Delta S^{\circ}_{ads}$ J $mol^{-1}K^{-1}$
303	42.91	19.59		86.27
308	29.59	18.65		86.91
313	25.51	18.28	45.73	85.77
318	23.15	18.04		84.28
323	17.15	17.81		84.55

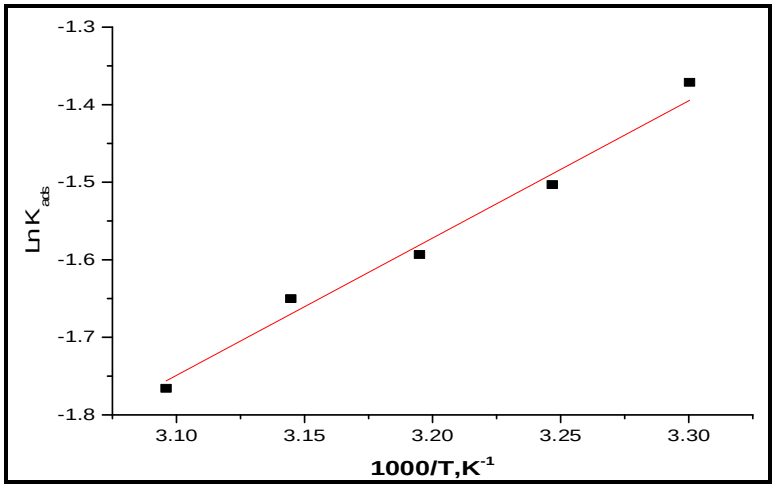

Figure 9. Graph of ($ln\ K_{ads}$) against (1000/*T*) for the dissolution of HCS in 1M HCl solution + *OME*

Kinetic-thermodynamic corrosion parameters: The parameters of activation for dissolution procedure measured from Arrhenius plot as below:

$$\log k = \frac{-E_a^*}{2.303\ R\ T} + \log A \qquad \ldots(7)$$

E^*_a can be gotten from the slope of log (k_{corr}) against 1/T plots with and without various doses of the OME as shown in (Figure 10). Data of E_a^* are reported in (Table 7). Examination of the data showed that E_a^* has higher values in the existence of the OME than that in its absence. This has attributed the physical adsorption of OME on HCS surface [**49**]. The transition state theory was used to compute the entropy and enthalpy of activation (Figure 11):

The values of change of entropy (ΔS^*) and change of enthalpy (ΔH^*) can be calculated by using the formula:

$$k = \left(\frac{RT}{Nh}\right) exp\left(\frac{\Delta S^*}{R}\right) exp\left(\frac{\Delta H^*}{RT}\right) \qquad \ldots(8)$$

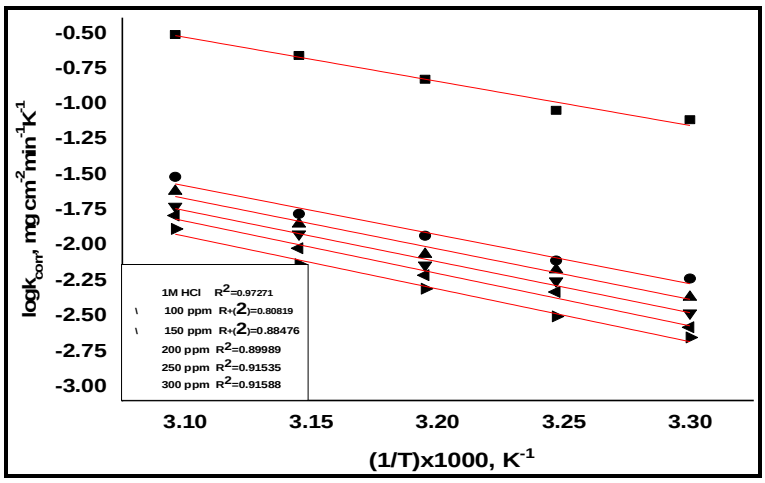

Figure 10. Log k_{corr} vs reciprocal of temperature plot for HCS non-using and using many OME contents.

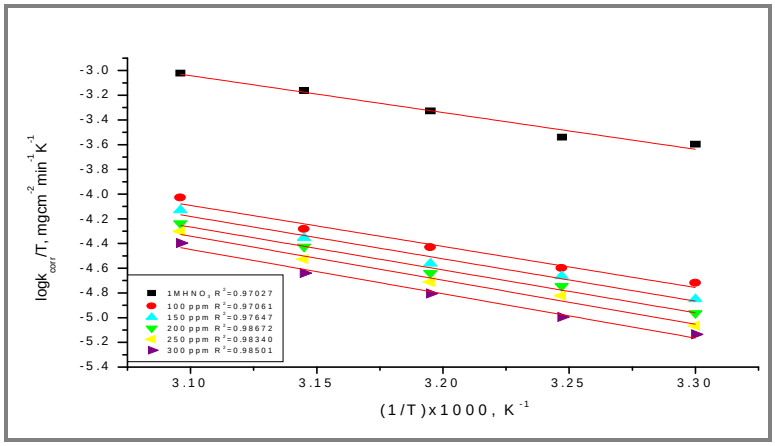

Figure 11. The relation between (log C.R. / T) and 1/ T diagrams for the HCS without and with several OME doses.

Table 7. Data of activation for HCS without and with range of OME doses

Conc. ppm	Ea* , kJ mol^{-1}	Δ H*, kJ mol^{-1}	-ΔS*, J mol^{-1}K^{-1}
1.0 M HCl	56.4	24.7	74.2
100	66.2	27.6	73.3
150	68.2	28.4	69.1
200	69.1	28.8	69.8
250	70.8	29.6	74.2
300	71.2	29.8	73.3

FTIR spectra Analysis: FTIR test established on analyzing the coated film found on the HCS surface [50-54]. In figure 12 demonstrations the FTIR of the pure OME and metal surface. The – N –H stretching frequency seems at 3325 cm^{-1} with medium intensity and broad band. The – O –H stretching frequency of the alcohol group seems at 3563 cm^{-1} which has strong and broad intensity [55-57]. The – C–O frequency appears at 1068 cm^{-1} with medium intensity. The –C=C–frequency appears at 1627 cm^{-1} with medium intensity also. At 1458 cm^{-1} strong band appears which indicating the aromatic ring in pure OME. The –O–H of carboxylic acid group stretching frequency seems at 2939 cm^{-1} with strong and very broad band.

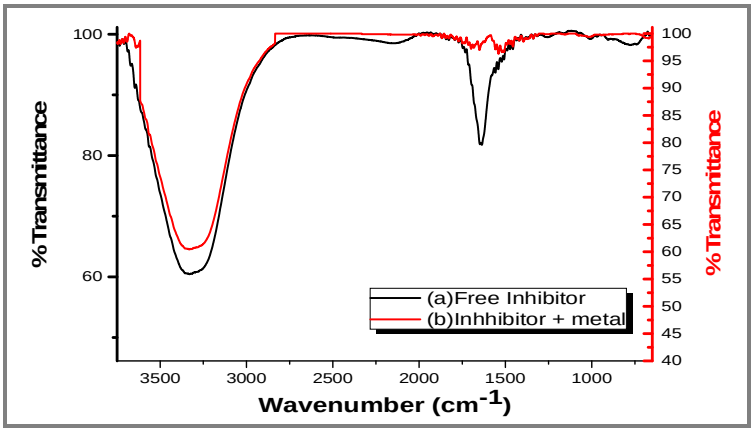

Figure 12. FTIR spectrum.

Figure 12 show FTIR spectra of the film designed on the HCS after dipping in a solution enclosing OME. The FTIR the formed film on the HCS surface, after dipping in solution including 1M HCl containing and 300 ppm of OME, is displayed in (Figure 12). The N –H frequency has moved from 3325 cm^{-1} to 3361 cm^{-1} with two medium bands. The – O –H frequency has moved from one band to make two free and sharp bands at 3566 and 3589 cm^{-1} with strong intensity. The – C–O frequency has moved from 1068 cm^{-1} to 1016 cm^{-1} with strong intensity. The –C=C–frequency has moved from 1627 cm^{-1} to 1650 with medium intensity also The –O–H of carboxylic acid group stretching frequency shifted from 2939 cm^{-1} to 2982 with strong and very broad band also. The study FTIR spectral demonstrations the formation of the protective film consists of Fe^{2+}-OME complex [**58-60**].

Surface studies by scanning electron microscopy (SEM): To evaluate the exchanges of the HCS surface engaging in acid solution with the absence and attendance of inhibitor OME. The HCS surface was analyze by using SEM. The HCS surface is more degradation due to corrosion attack in the blank solution. Figure 13, suggests the micrograph given for HCS sheets in absence and using 300 ppm of OME after dipping for only one day The OME adsorption on the HCS surface, forming the shielding layer resulting in blocking the surface active areas so that the surface become more smooth and protection [**61**].

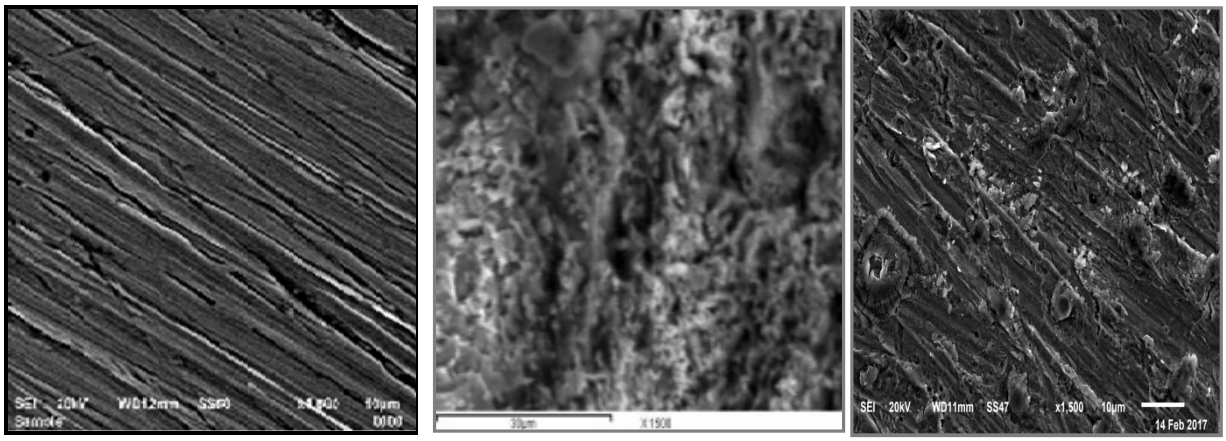

(a) (b) (c)

Figure 13. SEM photo of HCS surface (a) before of soaking in 1 M HCL, (b) after 12 h of soaking in 1.0 M HCL and (c) after 12 h of soaking in 1 M HCL + 300 ppm of OME at 25°C.

Energy dispersion spectroscopy (EDX) studies: Figure 14a displays the EDX investigation result on the composition of HCS only without the acid and inhibitor usage. The EDX study designates that only Fe and oxygen were obtaining, which demonstrations that the passive film confined only Fe_2O_3. Figure 14b Portrays the EDX analysis of HCS in 1 M HCl only and figure 14c shows EDX displays the EDX analysis of HCS in 1 M HCl in the attendance of 300 ppm of OME. The spectra display additional lines, demonstrating the attendance of C (owing to the carbon atoms of OME). The data illustrations that the C and N materials coated the HCS surface. A comparable elemental distribution is revealed in (Table 8).

Table 8. Mass % of HCS after 12h of dipping in HCl without and with the 300-ppm dose of the OME

(Mass %)	Fe	Cl	C	O	Tb
High carbon steel	78.51	--	9.19	3.05	9.26
Blank	81.22	--	8.35	--	10.43
OME	74.16	0.40	8.34	8.10	9.0

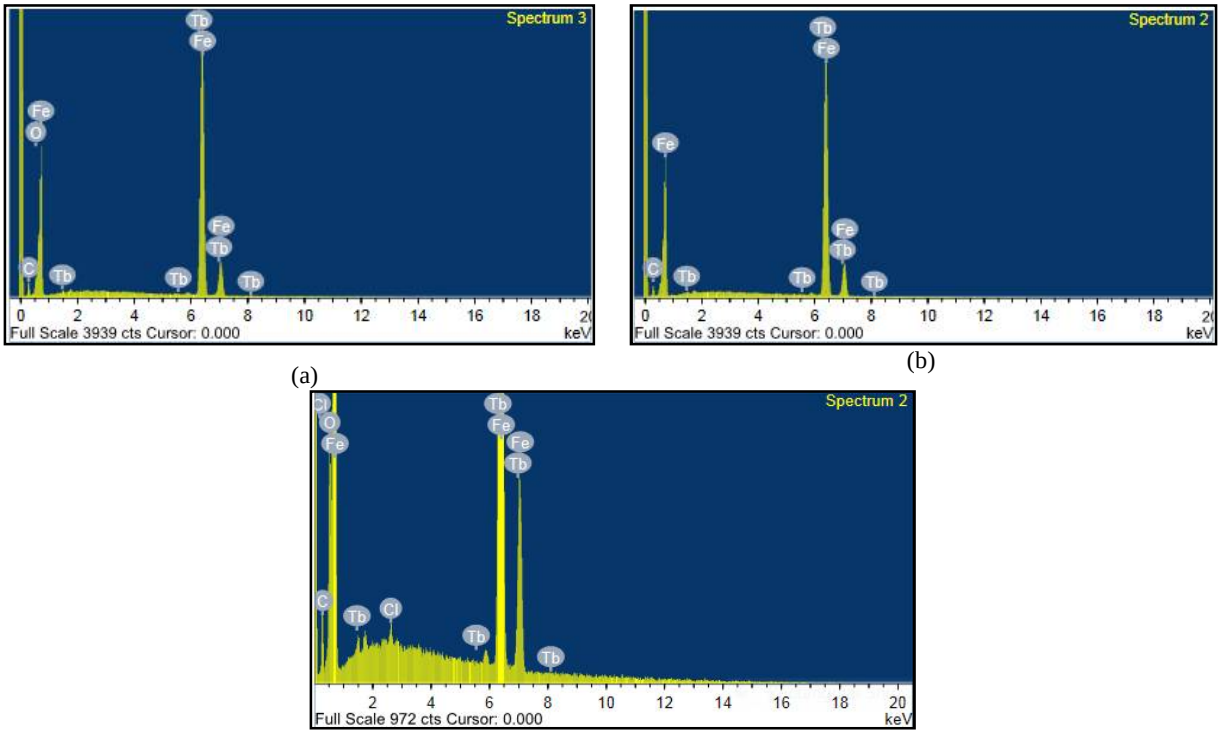

Figure 14 (a). EDX analysis on HCS (free) (b). Blank of HCS in1.0M HCl (c). HCS soaking in 1.0M HCl with the attendance of OME for 12 Hours**.**

AFM Characterization: This method gives a map about the metal surface where roughness is indicating with an excessive resolve [**62**]. The 3D images of AFM shown in figure 15.

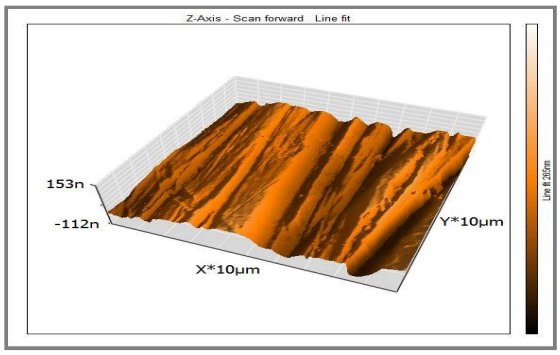

Free

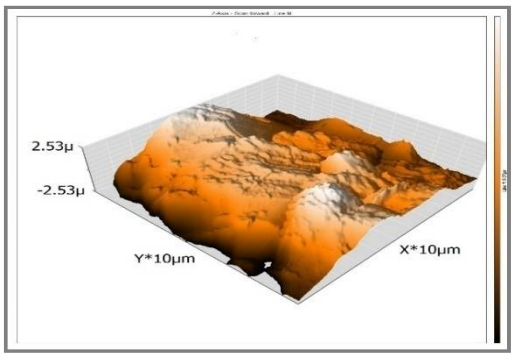

Blank

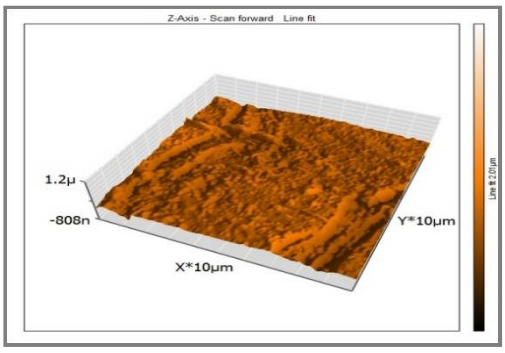

300ppm OME Compound

Figure15. (3D) AFM images of HCS without acid (free), HCS in 1.00M HCl (blank), and HCS in 1.00 M HCl at 300 ppm of OME for 24 hours at 25^{o}C.

Table 9. AFM data for HCS surface with and without OME environment.

Sample	Sa	Sq	Sp
Free	20.63	24.79	60.26
Blank	694.9	810.95	1830.2
OME inhibitor	59.744	77.544	391.28

From the table, the surface of the HCS is smoother than in the presence of the OME as a result of OME adsorption therefore the acid attack is reduced.

Theoretical studies: Some calculations of quantum studies can be carried out to examine the impact of ring structure of OME inhibitor to study the productivity of hindrance mechanism. Bond lengths and bond angles can be optimized to obtain the geometric and electronic structure of the OME inhibitor figure 16a displays the molecular structures optimized of the OME inhibitor. We enlarged some data from the quantum parameter for investigated OME inhibitor as:

Highest occupied molecular orbital ($\mathbf{E_{HOMO}}$) = - 4.63 eV, Lowest unoccupied molecular orbital ($\mathbf{E_{LUMO}}$) = 2.2 eV, Energy gap $\mathbf{\Delta E}$ = 6.83 eV, Dipole moment ($\boldsymbol{\mu}$) = 13.45 Debye.

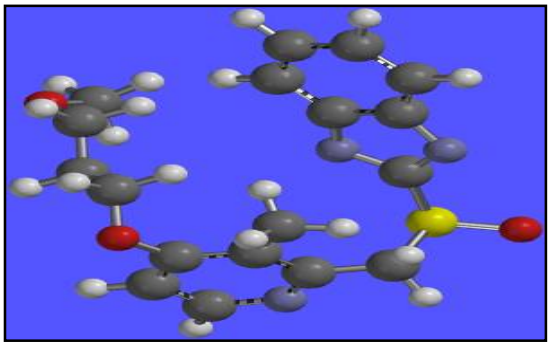

Figure (16.a). Optimized molecular structure with Mullikan atomic charges of OME inhibitor

E_{HOMO} is related to the electron donating ability of the molecule. The high value of E_{HOMO} is pointed to a tendency of the molecule to give electrons to be suitable for the molecules acceptor which devising small energy and empty molecular orbitals [**63**]. The protection efficiencies improve with the upper or less negative E_{HOMO} energies, with raising data of the dipole moment with diminishing the data of ΔE (energy gap) [**64, 65**] and the stronger interaction between inhibitors and metal surface. Figure 16b shows great data of the HOMO density were found in the vicinity of S and N atoms, pointing to the nucleophilic center is the S and N atoms.

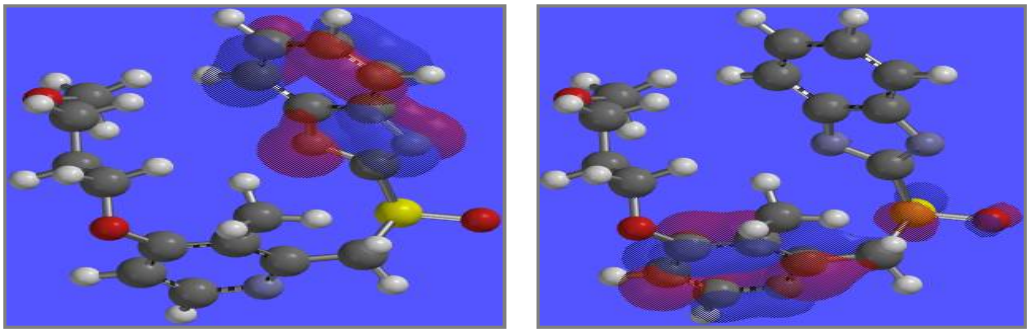

HOMO LUMO

Figure 15b. Optimized HOMO and LUMO structure of OME inhibitor.

Inhibition Mechanism: OME drugs inhibition for HCS corrosion in 1.0 M HCl solution had depend on the temperature, chemical structure and OME dose. By raising OME inhibitor dose, we founded some changes as; lowering of mass reduction, increment of resistance charge transfer, lowering of corrosion current, and higher of IE. Influence the adsorption procedure of OME on the HCS surface by some factors as molecular size, attendance of active sites in the chemical structure of OME, charge density and capability to form complexes. The inhibition action of this drug was attributed to blocking the surface via formation of insoluble complexes on metal surface [**66**]. The participation of hetero molecules in the OME structure drives its adsorption technique for foundation of coordinate bonds among the transfer of lone pairs of electrons of heteroatoms to the Fe surface these classes can adsorbed by the HCS. On account of alluring powers between the -ve charged metal and the +ve charged OME inhibitor atoms.

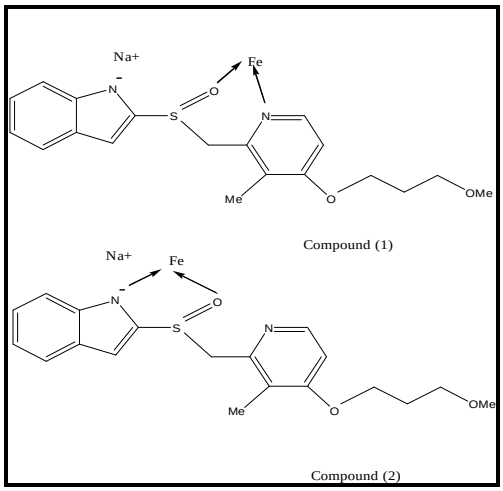

Figure 17. Two kinds of conceivable complexes for OME inhibitor.

Figure 17 shows that there are two kinds of possible complexes for OME inhibitor might be obtained. The compound (1) is steadier than compound (2) because of the development of chelated six membered rings with Fe atom. The compound (2) is less steady because of the arrangement of five membered rings. It notable that the six membered ring is steadier than the five membered rings.

APPLICATION

The use of this expired drug as corrosion inhibitors can solve two major environmental and economical problems.

CONCLUSION

Excellent inhibition for the OME inhibitor to the corrosion of HCS in 1.0M HCl system concluded adsorption interaction. The % I E is rise with improving the dose of OME and lowering temperature. The inhibition action of OME inhibitor is due to the creation of adsorbed insoluble complex on HCS. The adsorption procedure conforms Langmuir isotherm. The outcome data from EIS test runs parallel with PP tests. SEM and AFM analysis also prove the creation of protective film on the surface of HCS surface in 1.0 M HCl.

REFERENCES

[1]. J. F. Carpenter, M. A. Mcnulty, L. J. Dusci, K. F. Ilett, Stability of omeprazole sodium and pantoprazole sodium diluted for intravenous infusion, *J Pharm Tech.* **2006**, 22, 95–98

[2]. 2. M. Vaz-Da-Silva, A. I. Loureiro, T. Nunes, J. Maia, S. Tavares, A. Falcão, P. Silveira, L. Almeida, P. Soares-Da-Silva, Bioavailability and Bioequivalence of Two Enteric-Coated Formulations of Omeprazole in Fasting and Fed Conditions, *Clin Drug Invest*, **2005**, 25(6), 391–399
[3]. K. G.Tolman, S. W.Sanders, K. N.Buchi, The effects of oral doses of lansoprazole and omeprazole on gastric pH, *J Clin Gastroenterol*, **1997**, 24(2), 65-70
[4]. C. W. Howden, Clinical pharmacology of omeprazole, *Clinical Pharmacokinetics*, **1991**, 20 (1), 38–49
[5]. C. A. M. Stedman, M. L. Barclay, Review article: comparison of the pharmacokinetics, acid suppression and efficacy of proton pump inhibitors, *Aliment Pharmacol Ther.*, **2000**, 14, 963-978.
[6]. E. Cheng, Proton Pump Inhibitors for Eosinophilic Esophagitis, *Current Opinion in Gastro-enterology*, **2013**, 29 (4),416–420
[7]. L. Fuccio, M. E. Minardi, R. M. Zagari, D. Grilli, N. Magrini, Bazzoli, Franco, Meta-analysis: Duration of First-Line Proton-Pump Inhibitor–Based Triple Therapy for Helicobacter pylori Eradication, *Annals of Internal Medicine*, **2007**, 147 (8), 553–62.
[8]. G. Sachs, J. M. Shin, C. Briving, The pharmacology of the gastric acid pump: the H^+,K^+ ATPase, *Annu Rev Pharmacol Toxicol*, **1995**, 35, 277-305
[9]. R. Huber, B. Kohl, G. Sachs, Review article: the con-tinuing development of proton pump inhibitors with partic-ular reference to pantoprazole, *Aliment Pharmacol Ther* , **1995**, 9, 363-78.
[10]. R. Holm, D.P. Elder, Analytical advances in pharmaceutical impurity profiling, *Eur. J. Pharmaceut. Sci.*, **2016**, 87, 118-135.
[11]. G. Trabanelli, Whitney Award Lecture: Inhibitors-An Old Remedy for a New Challenge, *Corrosion*, **1991**, 47, 410-419.
[12]. D. N. Singh, A. K. Dey, Synergistic Effects of Inorganic and Organic Cations on Inhibitive Performance of Propargyl Alcohol on Steel Dissolution in Boiling Hydrochloric Acid Solution, *Corrosion*, **1993**, 49, 594-600.
[13]. G. Banerjee, S. N. Malhotra, Contribution to Adsorption of Aromatic Amines on Mild Steel Surface from HCl Solutions by Impedance, UV, and Raman Spectroscopy**,** *Corrosion*, **1992**, 48, 10-15.
[14]. S. T. Arab, E. A. Noor, Inhibition of Acid Corrosion of Steel by Some S-Alkylisothiouronium Iodides, *Corrosion*, **1993**, 49, 122-129.
[15]. I. A. Raspini, *Corros.*, **1993**, 49, 821-829
[16]. A. Khadraoui, A. Khelifa, L. Touafri, H. Hamitouche, R. Mehdaoui, Influence of Sodium Salts of Organic Acids as Additives on Localized Corrosion of Aluminum and Its Alloys, *J. Mater. Environ. Sci.*, **2013**, 4, 663-828.
[17]. M. Elachouri, M. S. Hajji, M. Salem, S. Kertit, R. Coudert, E. M. Essassi., Some surfactants in the series of 2-(alkyldimethylammonio) alkanol bromides as inhibitors of the corrosion of iron in acid chloride solution, *Corros. Sci.*, **1995**, 37, 381-389.
[18]. H. Luo, Y. C. Guan, K. N. Han, Inhibition of Mild Steel Corrosion by Sodium Dodecyl Benzene Sulfonate and Sodium Oleate in Acidic Solutions, *Corrosion*, 1998, 54, 619-627.
[19]. M. A. Migahed, E. M. S. Azzam, A. M. Al-Sabagh, Corrosion inhibition of mild steel in 1 M sulfuric acid solution using anionic surfactant, *Mater. Chem.Phys*, **2004**, 85, 273-279.
[20]. R. F. V.Villamil, P. Corio, J. C. Rubim, M. L. S. Agostinho, Effect of sodium dodecylsulfate on copper corrosion in sulfuric acid media in the absence and presence of benzotriazole, *J. Electroanal. Chem.*, **1999**, 472, 112-119.
[21]. H. Kumar, S. Karthikeyan., Inhibition of mild steel corrosion in hydrochloric acid solution by cloxacillin drug, *J. Mater. Environ. Sci.*, **2012**, 3(5), 925-934.
[22]. H. Bendaha, A. Zarrouk, A. Aouniti, B. Hammouti, Adsorption and corrosion inhibitive properties of some tripodal pyrazolic compounds on mild steel in hydrochloric acid systems, *Phys. Chem. News*, **2012**, 64, 95-103.

[23]. A. S Fouda, A. El-Hossiany, H. Ramadan, Calotrpics procera plant extract as green corrosion inhibitor for 304 stainless steel in hydrochloric acid solution, *Zastita Materijala*, **2017**, 58(4), 541-555.
[24]. R. Guo, T. Liu, X. Wei, Effects of SDS and some alcohols on the inhibition efficiency of corrosion for nickel, *Colloids Surf A*, **2002**, 209, 37-45.
[25]. V. Branzoi, F. Golgovici, F. Branzoi, Aluminium corrosion in hydrochloric acid solutions and the effect of some organic inhibitors, *Mater. Chem. Phys.*, **2002**, 78, 122-131.
[26]. K. S. Parikh, K. J. Joshi, Natural compounds onion, garlic and bitter gourd as corrosion inhibitors for mild steel in hydrochloric acid, Trans. SAEST, **2004**, 39, 29-35.
[27]. A. S Fouda, A. El-Hossiany, H. Ramadan, Corrosion Inhibition of Rumex Vesicarius Extract on Stainless Steel 304 in Hydrochloric Acid, *IJRASET*, **2017**, 5, 1698-1710.
[28]. S. S. Abd El Rehim, H. Hassan, M. A. Amin, The corrosion inhibition study of sodium dodecyl benzene sulphonate to aluminium and its alloys in 1.0 M HCl solution, *Mater. Chem. Phys.*, 2003, 78, 337-348.
[29]. A. S. Fouda, M. Abdel Azeem, S. A. Mohamed, A. El-Hossiany and E. El-Desouky, Corrosion Inhibition and Adsorption Behavior of Nerium Oleander Extract on Carbon Steel in Hydrochloric Acid Solution, *Int. J. Electrochem. Sci.*, **2019**, 14, 3932-3948.
[30]. D. Q. Zhang, Q. R. Cai, X. M. He, L. X. Gao, G. S. Kim, Corrosion inhibition and adsorption behavior of methionine on copper in HCl and synergistic effect of zinc ions, *Mater. Chem. Phys.*, **2009**, 114, 612-617.
[31]. J. O. Bockris, D. A. J. Swinkels, Adsorption of n-decylamine on solid metal electrodes, J. Electrochem. Soc.**, 1964**, 111,736-747.
[32]. M. M. Saleh, A. A. Atia, Effects of structure of the ionic head of cationic surfactant on its inhibition of acid corrosion of mild steel, *J. Appl. Electrochem.*, **2006**, 36, 899-905.
[33]. L. Narvez, E. Cano, D. M. Bastidas, 3-Hydroxybenzoic acid as AISI 316L stainless steel corrosion inhibitor in a H 2 SO 4–HF–H 2 O 2 pickling solution, *J. Appl. Electrochem.*, **2005**, 35, 499-506.
[34]. X. H. Li, S. D. Deng, H. Fu, Synergism between red tetrazolium and uracil on the corrosion of cold rolled steel in H2SO4 solution, *Corros. Sci.*, **2009**, 51, 1344-1355.
[35]. V. R. Saliyan, A. V. Adhikari, Inhibition of corrosion of mild steel in acid media by N′-benzylidene-3-(quinolin-4-ylthio) propanohydrazide, *Bull. Mater. Sci*., **2008**, 31, 699-711.
[36]. L. Li, X. Zhang, J. Lei, J. He, S. Zhang, Adsorption and corrosion inhibition of Osmanthus fragran leaves extract on carbon steel, *Corrosion Science*, **2012**, 63, 82-90.
[37]. E. S. Ferreira, C. Giacomelli, F. C. Giacomelli, A. Spinelli, Evaluation of the inhibitor effect of L-ascorbic acid on the corrosion of mild steel, *Mater. Chem.Phys*., **2004**, 83, 129-134.
[38]. H. P. Lee, K. Nobe, Kinetics and mechanisms of Cu electrodissolution in chloride media, *J. Electrochem. Soc*., **1986**, 133, 2035-2043.
[39]. F. Mansfeld, Recording and analysis of AC impedance data for corrosion studies, *Corros.*, 1981, 36, 301-307.
[40]. C. Gabrielli, "Identification of Electrochemical processes by Frequency Response" *Analysis Solarton Instrumentation Group*, **1980**.
[41]. M. El Achouri, S. Kertit, H. M. Gouttaya, B. Nciri, Y. Bensouda, L. Perez, M. R. Infante, K. Elkacemi, Corrosion inhibition of iron in 1 M HCl by some gemini surfactants in the series of alkanediyl-α, ω-bis-(dimethyl tetradecyl ammonium bromide), *Prog. Org. Coat*., **2001**, 43, 267-273.
[42]. J. R. Macdonald, W. B. Johanson, In: J.R. Macdonald (Ed.), Theory in Impedance Spectroscopy, John Wiley& Sons, *New York*, **1987**.
[43]. S. F. Mertens, C. Xhoffer, B. C. Decooman, E. Temmerman, Short-term deterioration of polymer-coated 55% Al-Zn—part 1: behavior of thin polymer films, *Corros.*, **1997**, 53, 381-387.
[44]. G. Trabanelli, C. Montecelli, V. Grassi, A. Frignani, Electrochemical study on inhibitors of rebar corrosion in carbonated concrete, *J. Cem. Concr. Res*., **2005**, 35, 1804-1813.

[45]. M. M. Motawea, A. El-Hossiany, and A. S. Fouda, Corrosion control of copper in nitric acid solution using chenopodium extract, *Int. J. Electrochem. Sci.,* **2019**, 14, 1372-87.
[46]. F. M. Reis, H. G. de Melo, I. Costa, EIS investigation on Al 5052 alloy surface preparation for self-assembling monolayer, *J. Electrochem. Acta,* **2006**, 51, 1780-1788.
[47]. M. Lagrenee, B. Mernari, M. Bouanis, M. Traisnel, F. Bentiss, Study of the mechanism and inhibiting efficiency of 3, 5-bis (4-methylthiophenyl)-4H-1, 2, 4-triazole on mild steel corrosion in acidic media, *Corros. Sci.,* **2002**, 44, 573-588.
[48]. A.S Fouda, A. M. El-Wakeel, K. Shalabi and A. El-Hossiany, Corrosion Inhibition for Carbon Steel by Levofloxacin Drug in Acidic Medium, *J. Elixir Corrosion and Dye*, **2015**, 83, 33086-33094.
[49]. H. Ma, S. Chen, L. Niu, S. Zhao, S. Li, D. Li, Inhibition of copper corrosion by several Schiff bases in aerated halide solutions, *J. Appl. Electrochem.,* **2002**, 32, 65-72.
[50]. E. Kus, F. Mansfeld, An evaluation of the electrochemical frequency modulation (EFM) technique, *Corros. Sci.,* **2006**, 48, 965-979.
[51]. G. A. Caigman, S. K. Metcalf, E. M. Holt, Thiophene substituted dihydropyridines, *J. Chem. Cryst.,* **2000**, 30, 415-422.
[52]. S. S. Abdel–Rehim, K. F. Khaled, N. S. Abd–Elshafi, Electrochemical frequency modulation as a new technique for monitoring corrosion inhibition of iron in acid media by new thiourea derivative, *Electrochim. Acta,* **2006**, 51, 3269-3279.
[53]. S. Zhang, Z. Tao, W. Li, The effect of some triazole derivatives as inhibitors for the corrosion of mild steel in 1 M hydrochloric acid, *Appl Surf Sci.,* **2009**, 255, 6757-6763.
[54]. A. S. Fouda, K. Shalabi, A. El-Hossiany, Moxifloxacin Antibiotic as Green Corrosion Inhibitor for Carbon Steel in 1 M HCl, *J. Bio Tribo Corros.,* **2016**, 2,18.
[55]. R. Kalaivani, B. Narayanasamy, J. A. Selvi, Corrosion Inhibition by prussian blue, *Port Electrochim Acta.,* **2009**, 27, 177-187.
[56]. J. Sathiyabama, S. Rajendran, A. A. Selvi, Eosin as corrosion inhibitor for carbon steel in well water, *Open Corrosion J.,* **2009**, 2(1), 76-83.
[57]. A. S. Fouda, S. A. Abd El-Maksoud, A. El-Hossiany, A. Ibrahim, Corrosion Protection of Stainless Steel 201 in Acidic Media using Novel Hydrazine Derivatives as Corrosion Inhibitors, *Int. J. Electrochem. Sci.,* **2019**, 14, 2187-2207.
[58]. A. S. Fouda, M. Eissa, A. El-Hossiany, Ciprofloxacin as Eco-Friendly Corrosion Inhibitor for Carbon Steel in Hydrochloric Acid Solution, *Int. J. Electrochem. Sci.,* **2018**, 13, 11096-11112.
[59]. A. S. Fouda, H. Ibrahim, S. Rashwaan, A. El-Hossiany, R. M. Ahmed, Expired Drug (pantoprazole sodium) as a Corrosion Inhibitor for High Carbon Steel in Hydrochloric Acid Solution, *Int. J. Electrochem. Sci.,* **2018**, 13, 6327-6346.
[60]. S. Rajendran, B. V. Apparao, N. Palaniswamy, Synergistic effect of Zn^{2+} and ATMP in corrosion inhibition of mild steel in neutral environment, *Bull Electrochem.,* **1996**, 12, 15-19
[61]. A. S. Fouda, S. A. Abd El-Maksoud, A. A. M. Belal, A. El-Hossiany, A. Ibrahium, Effectiveness of Some Organic Compounds as Corrosion Inhibitors for Stainless Steel 201 in 1M HCl: Experimental and Theoretical Studies, *Int. J. Electrochem. Sci.,* **2018**, 13, 9826-9846.
[62]. P. Devi, J. Nithya, S. Sathiyabama, R. Rajendran, S. Prabha, Influence of citric acid-Zn^{2+} System on Inhibition of Corrosion of Mild Steel in Simulated Concrete Pore Solution, *Int J Nano Corr Sci and Engg,* **2015**, 2(3), 1-13.
[63]. A. S. Fouda, S. Rashwan, A. El-Hossiany, F. E. El-Morsy, Corrosion Inhibition of Zinc in Hydrochloric Acid Solution using some organic compounds as Eco-friendly Inhibitors, *JCBPS,* **2018**, 19(1)b, 001.
[64]. K. F. Kaled, K. Babic-Samardzij, N. Hackerman, Piperidines as corrosion inhibitors for iron in hydrochloric acid, *J. Appl. Electrochem.,* **2004**, 34, 697-704.
[65]. I. Lukovits, K. Palfi and E. Kalman, LKP model of the inhibition mechanism of thiourea compounds, *Corros.,* **1997**, 53, 915-919.
[66]. A. Popova. M. Christov, S. Raicheva, E. Sokolova, Adsorption and inhibitive properties of benzimidazole derivatives in acid mild steel corrosion, *Corros. Sci.,* **2004**, 46, 1333-1350.